

Lab Visualization and Medical Image Analysis  
Final Presentation

# The Impact of Fiber Orientation Features on Direct White Matter Tract Segmentation

---

March 15, 2024

Bertan Karacora  
Institute of Computer Science, University of Bonn  
[bertan.karacora@uni-bonn.de](mailto:bertan.karacora@uni-bonn.de)

# Contents

---

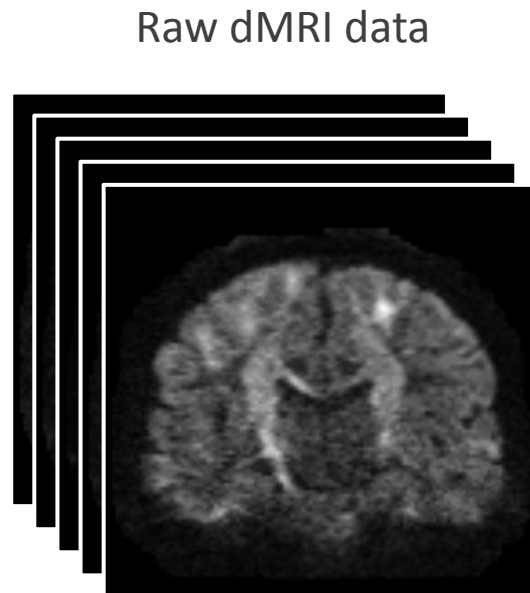
1. Introduction
2. Methods
3. Experiments and results
4. Discussion
5. Conclusion

# Contents

---

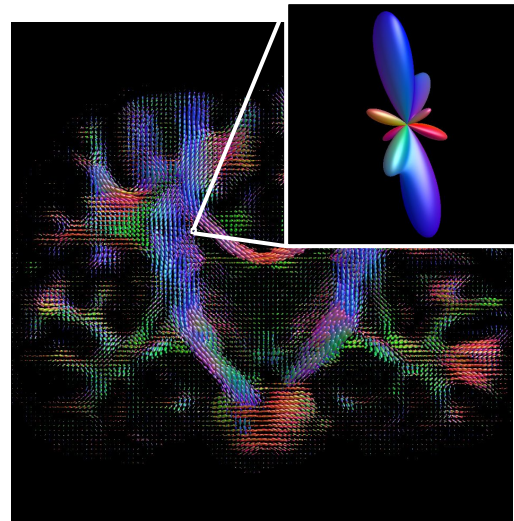
- 1. Introduction**
2. Methods
3. Experiments and results
4. Discussion
5. Conclusion

# Identifying white matter tracts



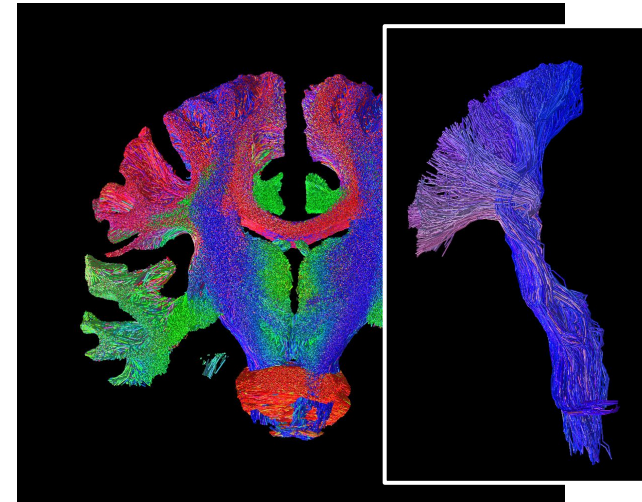
Tract identification difficult and strongly dependent on acquisition.

Fiber orientations (e.g., fODFs)



More condensed and robust representation but delineation hard for a human expert.

Tractogram (streamlines)



Identification from explicit global properties (ending regions, trajectory, ...).

**Figure 1:** Types of data for identifying white matter tracts. Left: Raw dMRI data contains all information but is susceptible to acquisition effects. Center: Local fiber orientations serve as abstraction of diffusion measurements. Right: Estimating fiber trajectories as streamlines makes more global properties explicit. Figure created by virtue of MRtrix3 [1] and Slicer3D [2].

➤ Tract identification = local information + spatial arrangement

# Applications

---

- Brain characterization, connectomics [4, 5]
- Neurosurgical planning (extend, position, shape of tracts) [6]
- Statistical analysis in tract areas or along their trajectory (tractometry [7])
- Guide tractography and segmentation of streamlines [8, 9, 10]

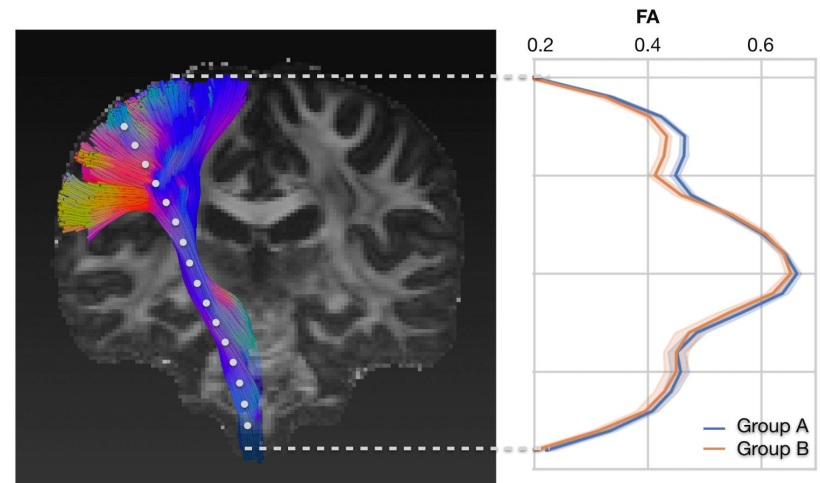


**Figure 3:** Concept image of tractometry. Fractional anisotropy (FA) is evaluated along streamlines of the CST tract. From [10].

# Direct tract segmentation

- Efficient voxel-wise labeling of tracts
- State-of-the-art CNN-based example: TractSeg [3]

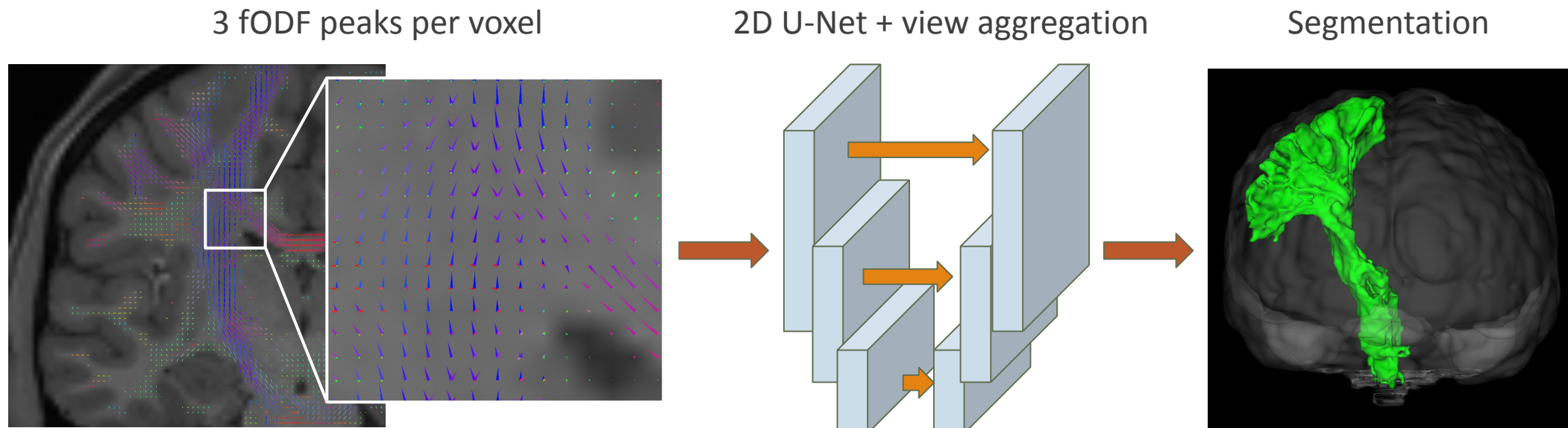


Figure 2: High-level view on TractSeg. A 2D CNN segments tracts in fields of fODF peaks. 2D Slices are aggregated to 3D. Figure created by virtue of MRtrix3 [1] and Slicer3D [2].

# Motivation of this project

---

- Address limitations of fODF peaks in TractSeg
  - Oversimplification of the fODF
  - Inherent directional ambiguity of 3D vector representation
  - Biases from interference
- Explore challenges and capabilities of alternative fODF features as model input

# Contents

---

1. Introduction
- 2. Methods**
3. Experiments and results
4. Discussion
5. Conclusion

# Overview

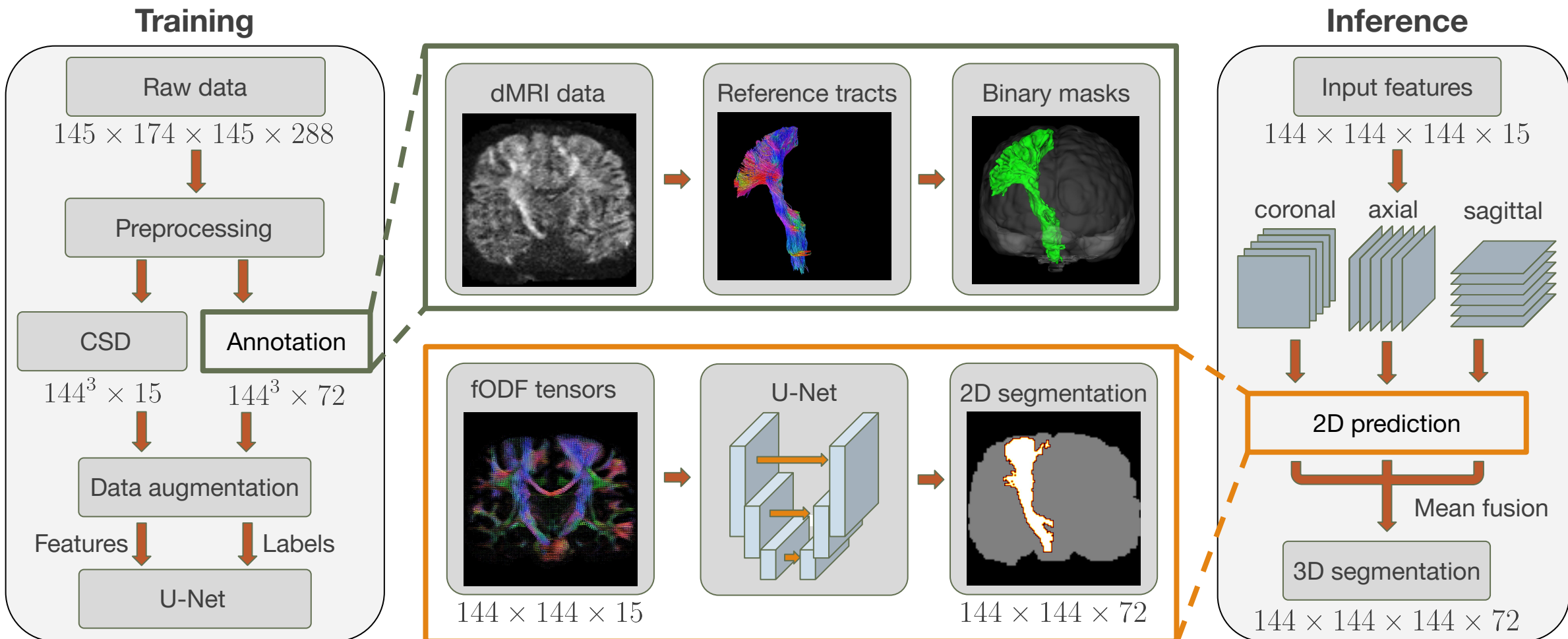


Figure 4: Method overview. The supervised training requires input features and reference labels from preprocessed data. During inference, the model predicts segmentations in 2D slices from coronal, axial, and sagittal directions, which are fused to 3D by averaging. The numbers below the boxes indicate the data dimensions after each step, exemplary for the case of fODF tensor inputs.

# Fiber orientation features

---

- Foundational idea: Constrained spherical deconvolution
- Voxel-wise representations
  - fODF as fourth-order tensor  $\mathcal{T} \in \mathbb{R}^{3 \times 3 \times 3 \times 3}$ 
    - Exploiting symmetry:  $T \in \mathbb{R}^{15}$
  - 3 fODF peaks (local maxima directions scaled by magnitude)
  - Rank-3 tensor approximation vectors  $\sqrt[4]{\lambda_i} \mathbf{v}_i$  from

$$\mathcal{T}^{(3)} = \sum_{i=1}^3 \lambda_i \mathbf{v}_i \otimes \mathbf{v}_i \otimes \mathbf{v}_i \otimes \mathbf{v}_i$$

# CNN architecture

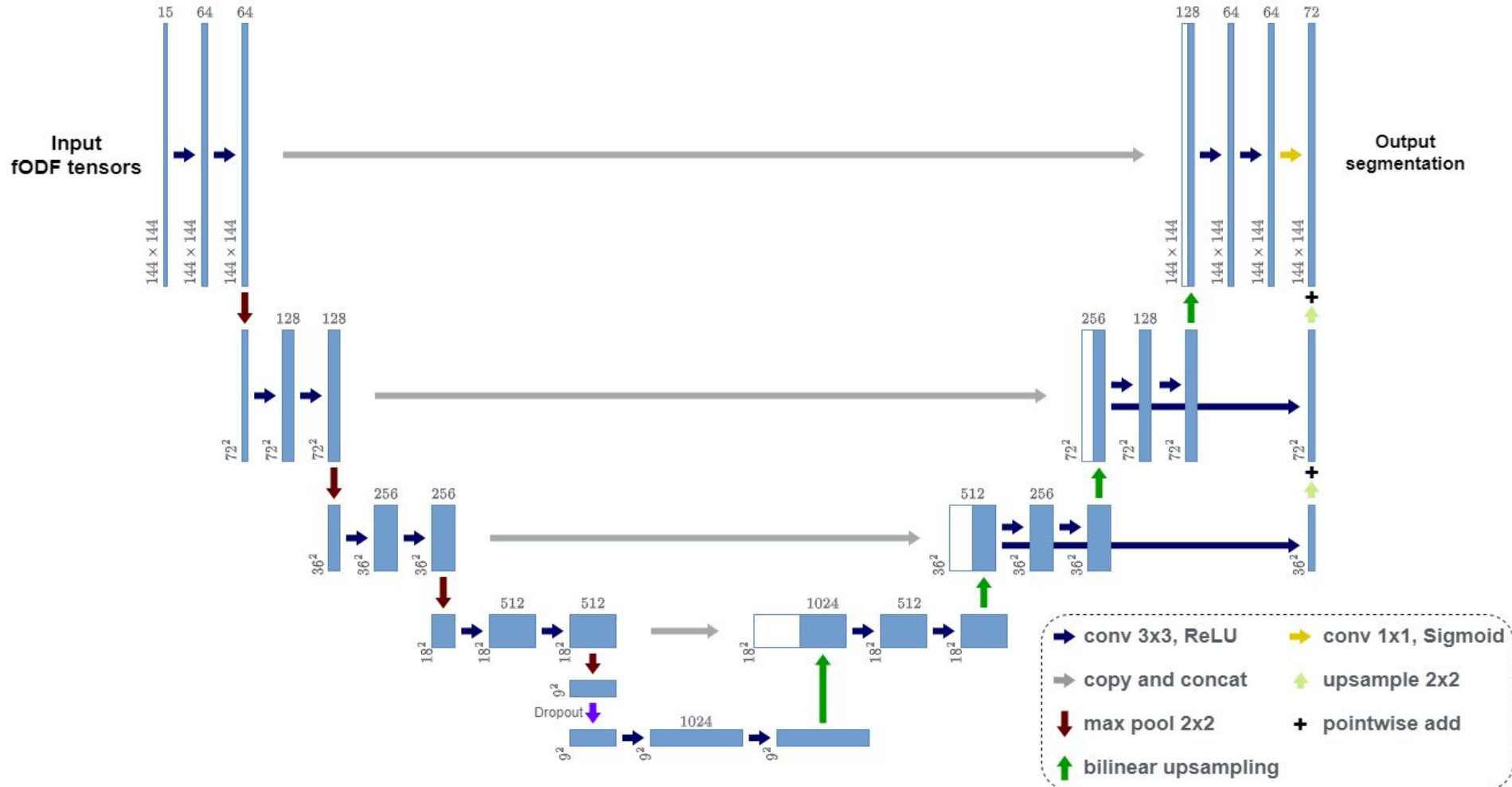


Figure 6: CNN architecture. Blue and white boxes represent generated and copied feature maps, respectively. Numbers denote their dimensions. Network operations are illustrated by the colored arrows and symbols shown at the bottom right. To learn from different fiber orientation such as fODF tensors, the channel width of the first convolutional layer is adapted to fit the feature dimension.

# Notable training details

---

- Cropping of features and labels to bounding box,  
padding to fixed input/output resolution  $144 \times 144$
- Uniform sampling of slicing axis and slices
- Slice normalization to zero mean and unit variance
- Binary cross-entropy loss

$$\text{loss}(\hat{y}, y) = -\frac{1}{72} \sum_{i=1}^{72} (y[i] \log(\hat{y}[i]) + (1 - y[i]) \log(1 - \hat{y}[i]))$$

# Data augmentation

---

- Transformations applied to each slice sample
  - Spatial: Rotation, displacement, scaling, elastic deformation
  - Noise: Gaussian blurring, additive Gaussian noise
- Key challenge: efficient implementation for fODF tensors
  - Scale standard deviation of Gaussian noise according to “multiplicity” of tensor components
  - Vectorize multilinear matrix product for rotation and sum coefficients corresponding to unique tensor components

# Contents

---

1. Introduction
2. Methods
- 3. Experiments and results**
4. Discussion
5. Conclusion

# Evaluation

---

- Fixed train-validation-test split of 105 subjects from the Human Connectome Project (HCP) [11]
- Best-epoch selection based on validation set performance
- Dice similarity coefficient per subject per tract:

$$\text{DSC}(\hat{V}_{s,t}, V_{s,t}) = \frac{2|\hat{V}_{s,t} \cap V_{s,t}|}{|\hat{V}_{s,t}| + |V_{s,t}|}$$

# Quantitative results - per test subject

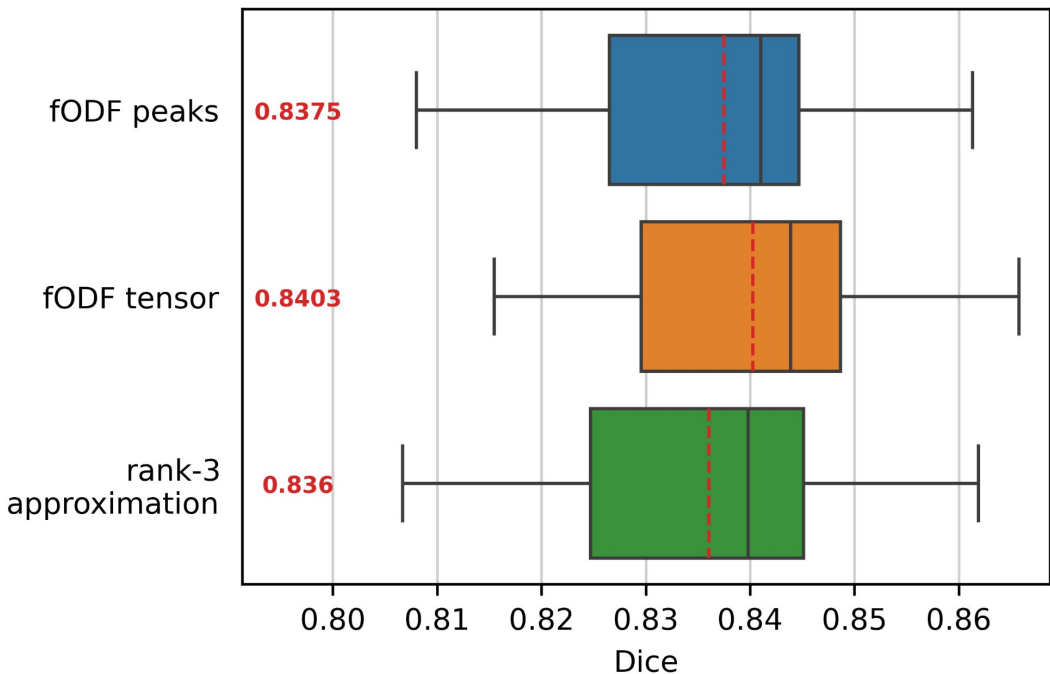


**Figure 7:** Comparison of segmentation accuracy using different fiber orientation features. The box plot shows the distributions of Dice scores (mean over all 72 tracts per subject). The mean across all test subjects scores is indicated by the dashed red line and the red number on the left.

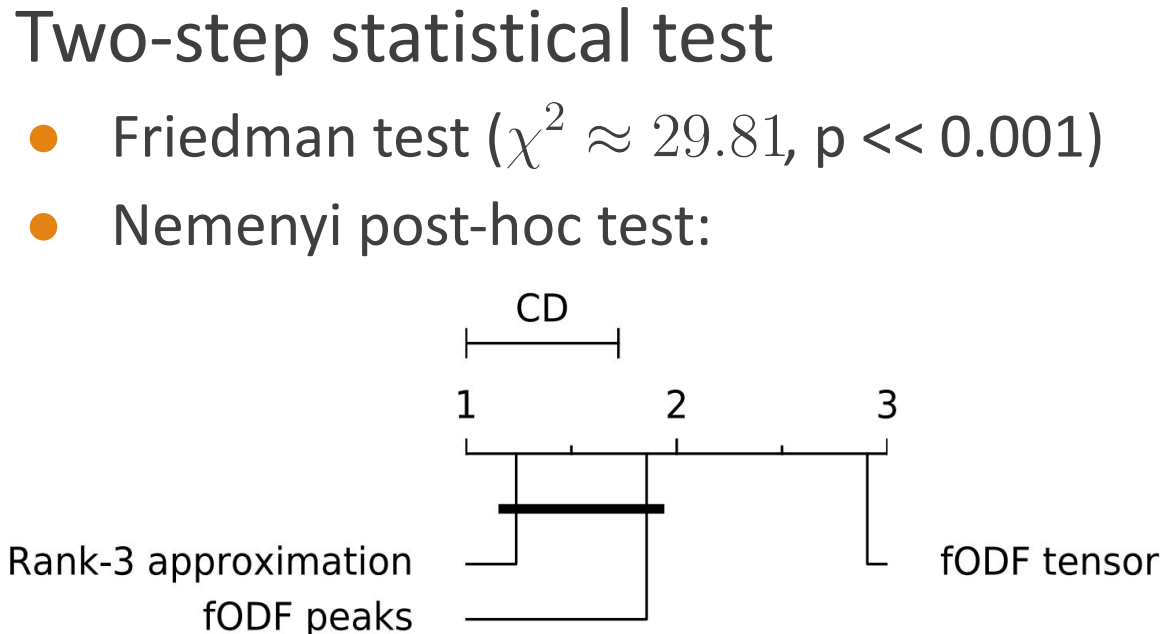


**Figure 8:** Critical distance diagram for the Nemenyi post-hoc test. A difference in the performance ranks larger than the critical distance (CD) indicates statistical significance (with  $p < 0.05$ ).

# Quantitative results - per tract

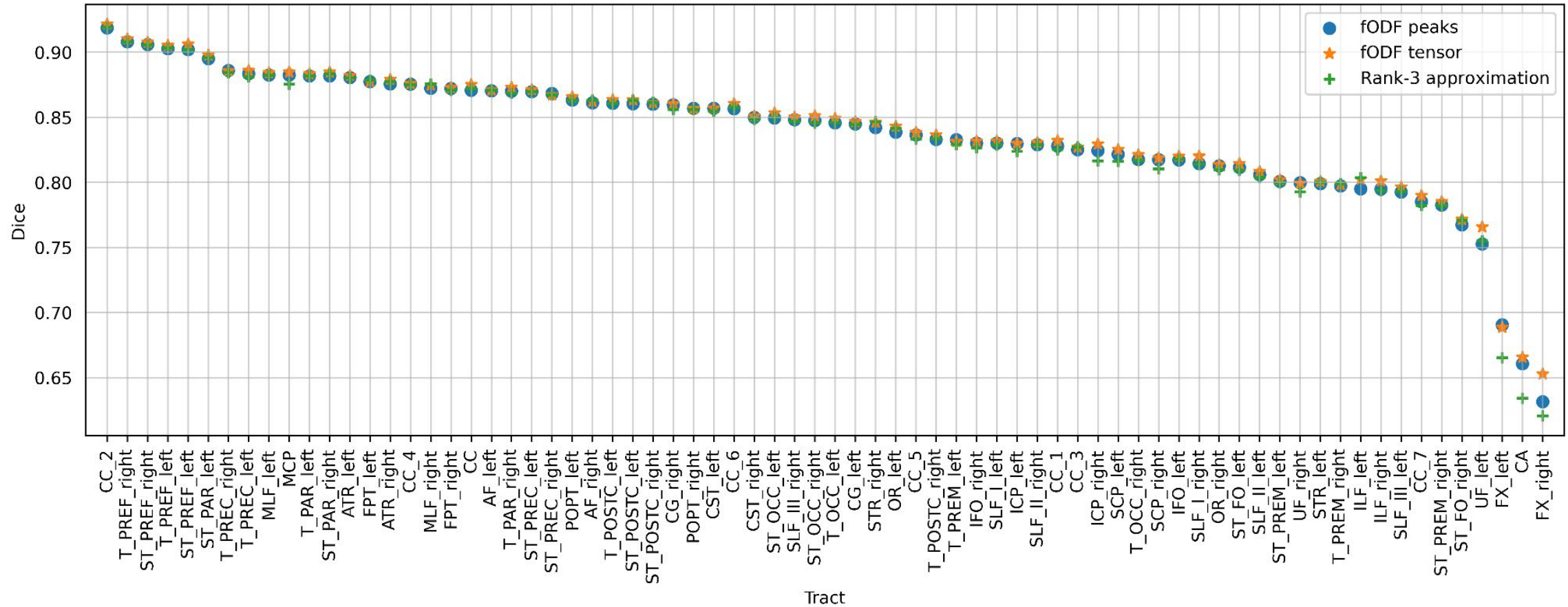
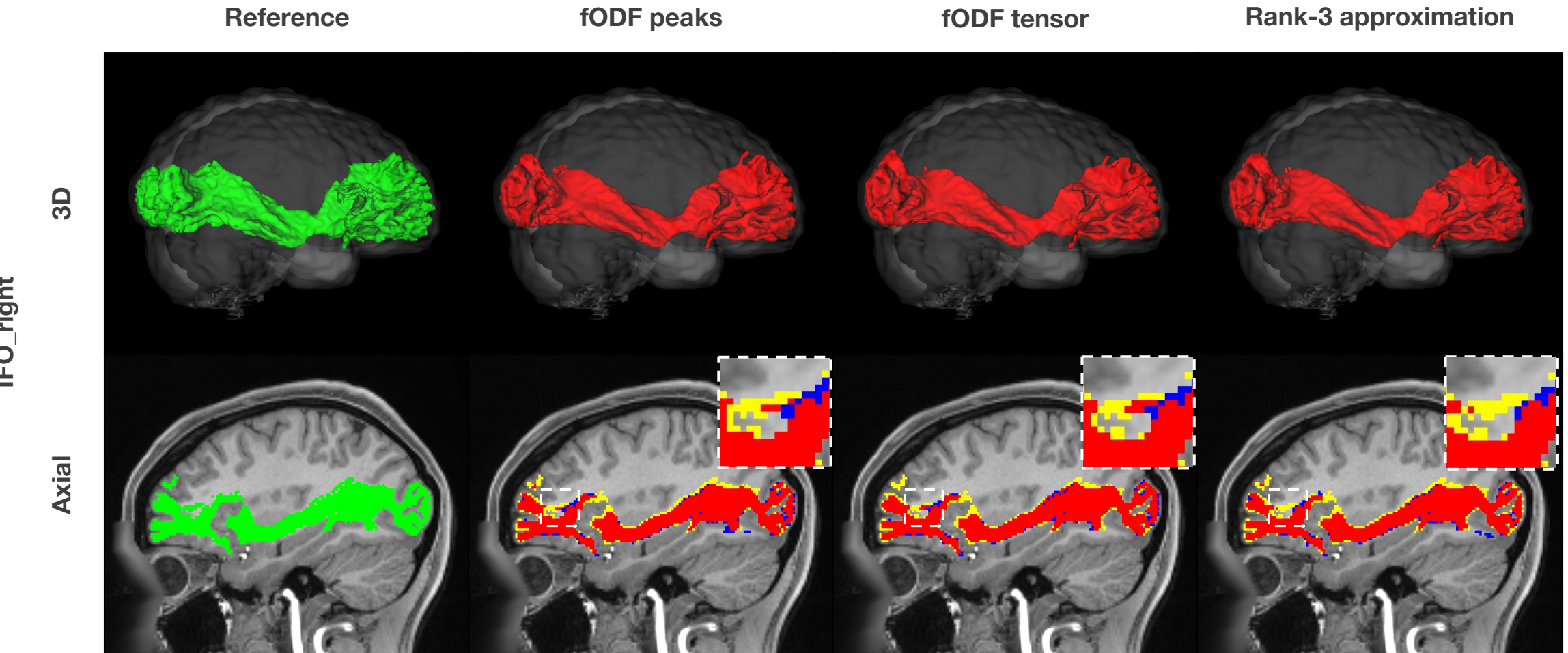


Figure 9: Mean Dice scores over all test subjects of each tract per model input.

# Qualitative results - IFO



**Figure 10:** Qualitative results using different fiber orientation features. Reconstruction of right inferior occipito-frontal fascicle (IFO\_right) of HCP subject 987983. Reference segmentation and model prediction are shown in green and red, respectively. Blue and yellow indicate false positives and false negatives, respectively. Figure created by virtue of MRtrix3 [1] and Slicer3D [2].

# Qualitative results - CST

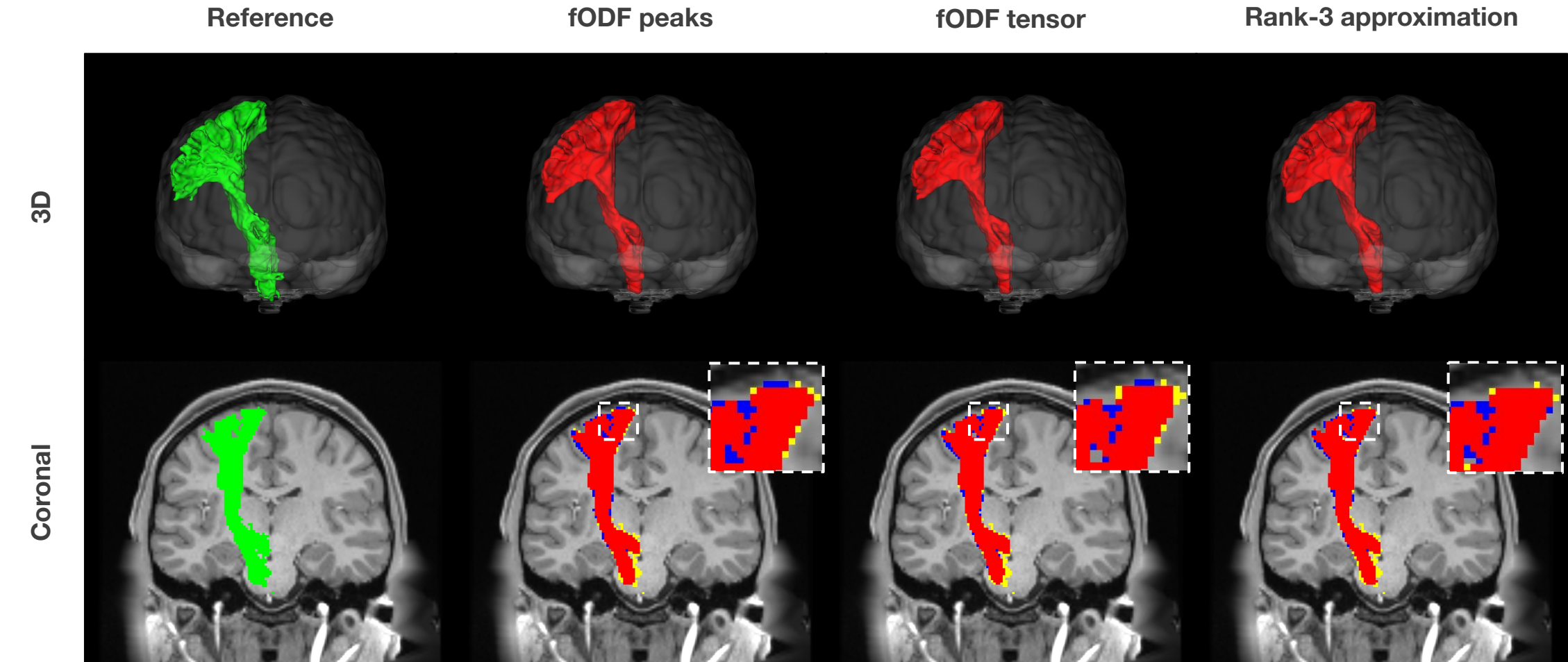


**Figure 11:** Qualitative results using different fiber orientation features. Reconstruction of right corticospinal tract (CST\_right) of HCP subject 987983. Reference segmentation and model prediction are shown in green and red, respectively. Blue and yellow indicate false positives and false negatives, respectively. Figure created by virtue of MRtrix3 [1] and Slicer3D [2].

# Qualitative results - CA

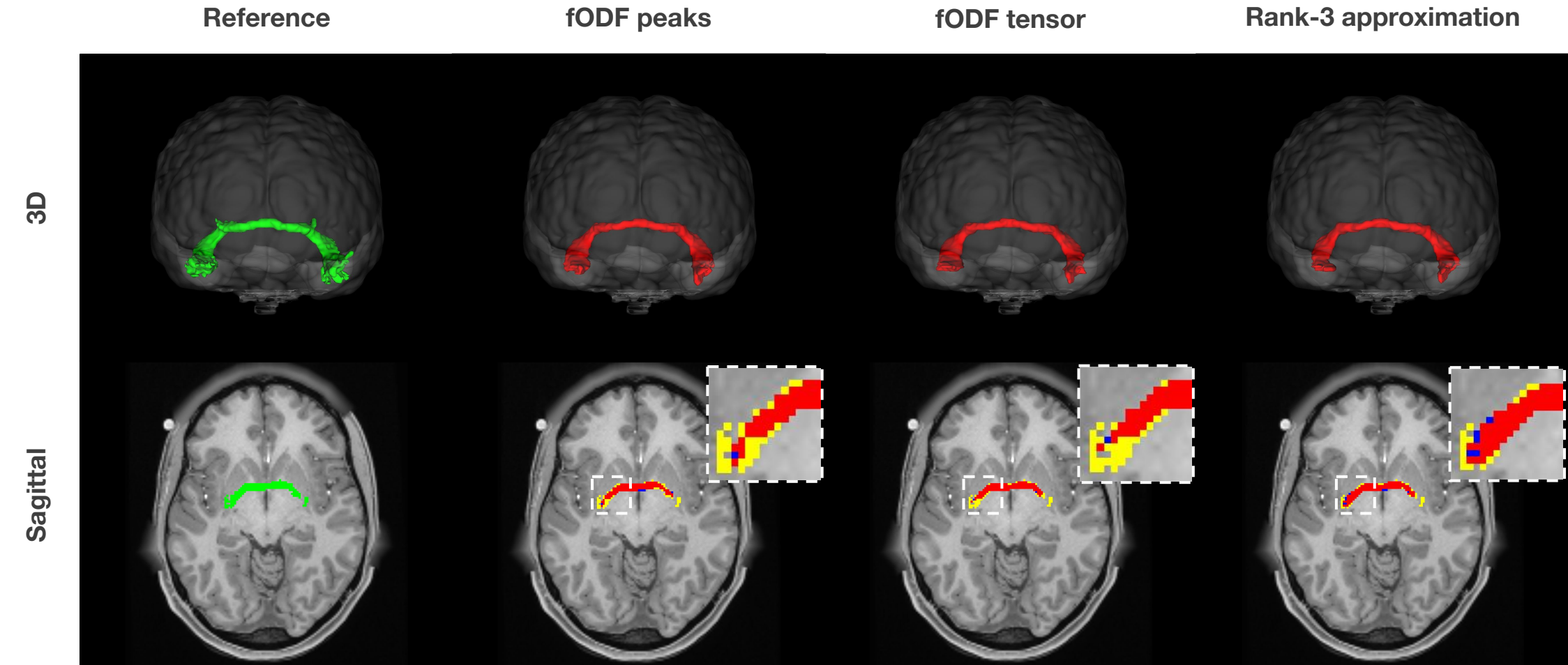


**Figure 12:** Qualitative results using different fiber orientation features. Reconstruction of commissure anterior (CA) of HCP subject 987983. Reference segmentation and model prediction are shown in green and red, respectively. Blue and yellow indicate false positives and false negatives, respectively. Figure created by virtue of MRtrix3 [1] and Slicer3D [2].

# Concatenation with structural features

---

- Additional experiment: Simple concatenation of
  - fODF tensors
  - a co-registered T1-weighted image
  - a partial volume map of the white matter
- Mean Dice score: approx. 0.8290
  - Conflicting information or fODF interpretation obstructed
  - Likely normalization issues

# Contents

---

1. Introduction
2. Methods
3. Experiments and results
- 4. Discussion**
5. Conclusion

# Limitations of fODF features

---

- Improvement from more comprehensive inputs small
  - Plus increased memory and training cost (inference cost negligible)
- No explicit description of overall fiber geometry
  - Difficulties from anatomical variability (e.g., tumors, lesions)
  - Lack of intuition for tract identification (vs. streamline segmentation)
  - Accounting for spatial arrangement requires inconvenient solutions like view aggregation
- Still affected by dMRI acquisition, assumptions and numerical errors of CSD methods

# Further developments and outlook

---

- TractSeg has highest degree of reproducibility among state-of-the-art methods (Schilling et al., 2021) [12]
- Improvements over TractSeg achieved for special applications
- Recent trend: direct segmentation using diffusion features or multi-modal inputs (e.g., AGYNet [13])
- Own observation: impact of fODF tensors most evident in difficult tract identification

➤ Fusion of dMRI-derived features with additional information.

# Contents

---

1. Introduction
2. Methods
3. Experiments and results
4. Discussion
- 5. Conclusion**

# Conclusion

---

- Local fODF expressive for efficient tract identification
- Example: TractSeg
  - CNN for spatial and more abstract features
  - High robustness
- fODF tensors improve over peaks by approx. 0.3 Dice points
- No significant effect from rank-3 approximations
- Prospective: combining dMRI-derived features with additional information

# References

In order of occurrence:

- [1] TOURNIER J.-D., SMITH R., RAAFFELT D., TABBARA R., DHOLLANDER T., PIETSCH M., CHRISTIAENS D., JEURISSEN B., YEH C.-H., CONNELLY A.: *MRtrix3: A fast, flexible and open software framework for medical image processing and visualisation.* Neuroimage 202 (2019), 116137.
- [2] FEDOROV A., BEICHEL R., KALPATHY-CRAMER J., FINET J., FILLION-ROBIN J.-C., PUJOL S., BAUER C., JENNINGS D., FENNESSY F., SONKA M., ET AL.: *3D Slicer as an image computing platform for the Quantitative Imaging Network.* Magnetic resonance imaging 30, 9 (2012), 1323–1341.
- [3] WASSERTHAL J., NEHER P., MAIER-HEIN K. H.: *TractSeg - Fast and accurate white matter tract segmentation.* NeuroImage 183 (2018), 239–253.
- [4] BULLMORE E., SPORNS O.: *Complex brain networks: graph theoretical analysis of structural and functional systems.* Nature reviews neuroscience 10, 3 (2009), 186–198.
- [5] MAIER-HEIN K. H., NEHER P. F., HOUDÉ J.-C., CÔTÉ M.-A., GARYFALLIDIS E., ZHONG J., CHAMBERLAND M., YEH F.-C., LIN Y.-C., JI Q., ET AL.: *The challenge of mapping the human connectome based on diffusion tractography.* Nature communications 8, 1 (2017), 1349.
- [6] YANG J. Y.-M., YEH C.-H., POUPON C., CALAMANTE F.: *Diffusion MRI tractography for neurosurgery: the basics, current state, technical reliability and challenges.* Physics in Medicine & Biology 66, 15 (2021), 15TR01.
- [7] BELLS S., CERCIGNANI M., DEONI S., ASSAF Y., PASTERNAK O., EVANS C., LEEMANS A., JONES D.: *Tractometry - comprehensive multi-modal quantitative assessment of white matter along specific tracts.* In Proc. ISMRM (2011), vol. 678.
- [8] WASSERTHAL J., NEHER P. F., MAIER-HEIN K. H.: *Tract orientation mapping for bundle-specific tractography.* In Medical Image Computing and Computer Assisted Intervention - MICCAI 2018: 21st International Conference, Granada, Spain, September 16-20, 2018, Proceedings, Part III 11 (2018), Springer, pp. 36–44.
- [9] WASSERTHAL J., NEHER P. F., HIRJAK D., MAIER-HEIN K. H.: *Combined tract segmentation and orientation mapping for bundle-specific tractography.* Medical image analysis 58 (2019), 101559.
- [10] WASSERTHAL J., MAIER-HEIN K. H., NEHER P. F., NORTHOFF G., KUBERA K. M., FRITZE S., HARNEIT A., GEIGER L. S., TOST H., WOLF R. C., ET AL.: *Multiparametric mapping of white matter microstructure in catatonia.* Neuropsychopharmacology 45, 10 (2020), 1750–1757.
- [11] VAN ESSEN D. C., SMITH S. M., BARCH D. M., BEHRENS T. E., YACOUB E., UGURBIL K., CONSORTIUM W.-M. H., ET AL.: *The WU-Minn human connectome project: an overview.* Neuroimage 80 (2013), 62–79.
- [12] SCHILLING K. G., TAX C. M., RHEAULT F., HANSEN C., YANG Q., YEH F.-C., CAI L., ANDERSON A. W., LANDMAN B. A.: *Fiber tractography bundle segmentation depends on scanner effects, vendor effects, acquisition resolution, diffusion sampling scheme, diffusion sensitization, and bundle segmentation workflow.* Neuroimage 242 (2021), 118451.
- [13] NELKENBAUM I., TSARFATY G., KIRYATI N., KONEN E., MAYER A.: *Automatic segmentation of white matter tracts using multiple brain MRI sequences.* In 2020 IEEE 17th International Symposium on Biomedical Imaging (ISBI) (2020), IEEE, pp. 368–371.

# Additional slides

---

# Supervision

High-quality tract dissections of 72 major white matter tracts provided by Wasserthal et al. [3]

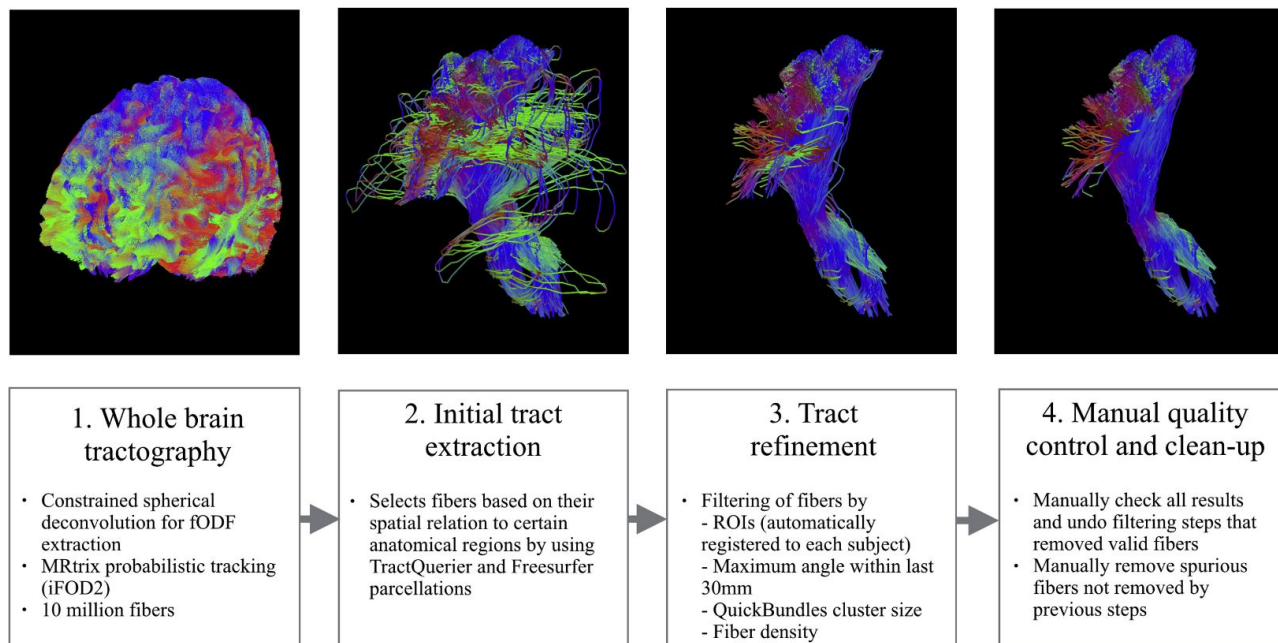


**Figure 5:** Semi-automatic dissection pipeline for creation of reference tracts. Images show the left CST of subject 898176. Adapted from [3].

# TractSeg - Overview with second FNN

- Segmentation of white matter tracts in dMRI
  - CNN approach based on U-net architecture
  - More accurate and faster than tractography-based methods

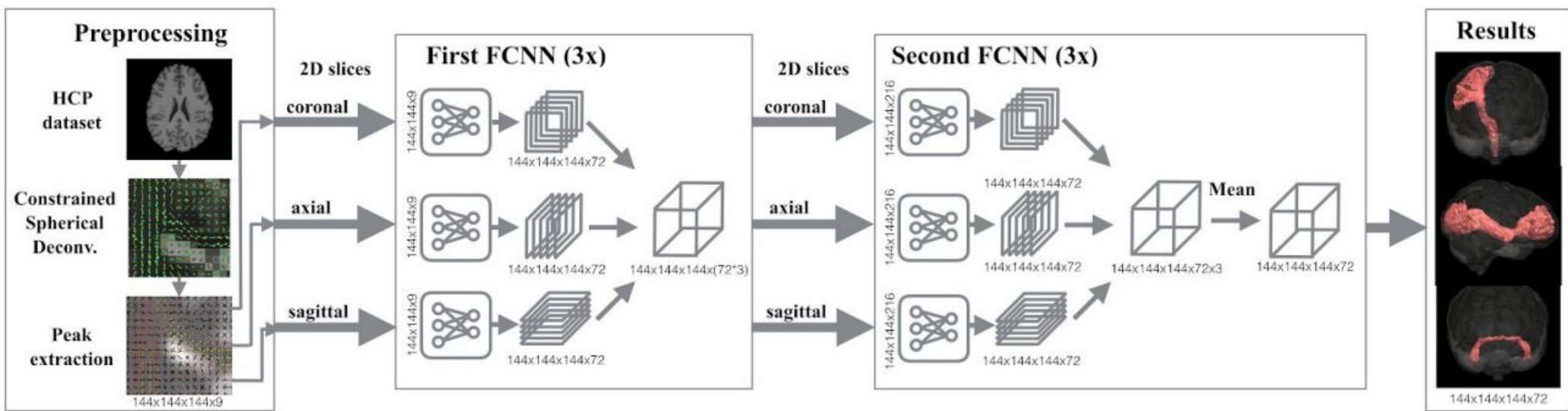


Image: Wasserthal et al., *NeuroImage* 2018]

# What happened to the second FCNN?

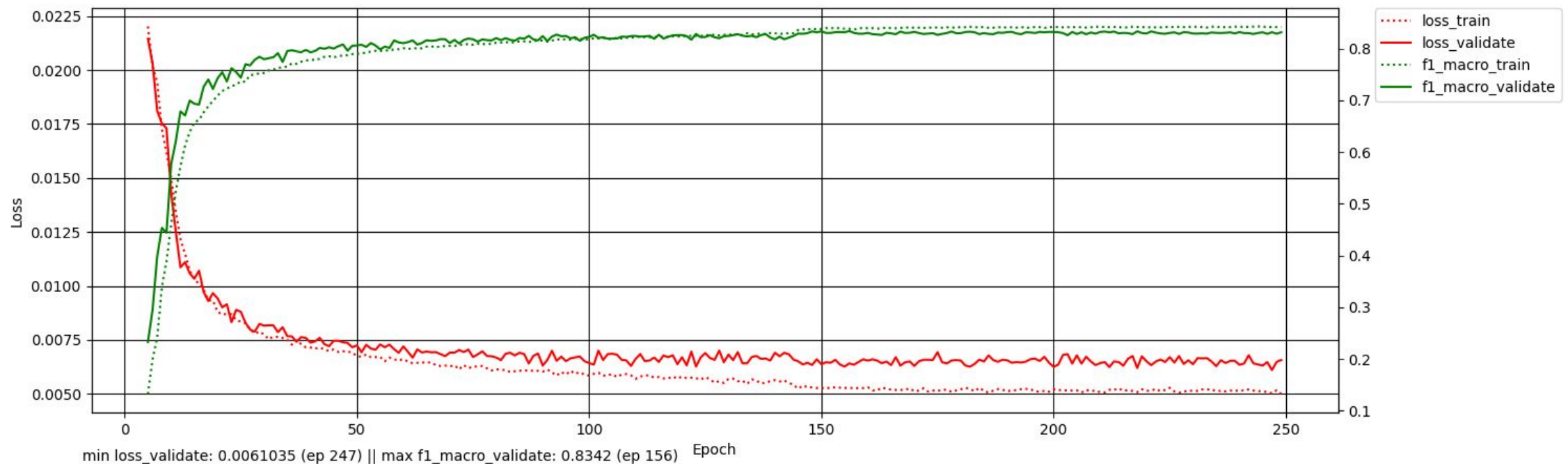
---

- Second CNN takes input slices with  $3 \cdot 72 = 216$  channels
  - Excessive increase of hardware requirements and training duration
- Jakob Wasserthal on GitHub:

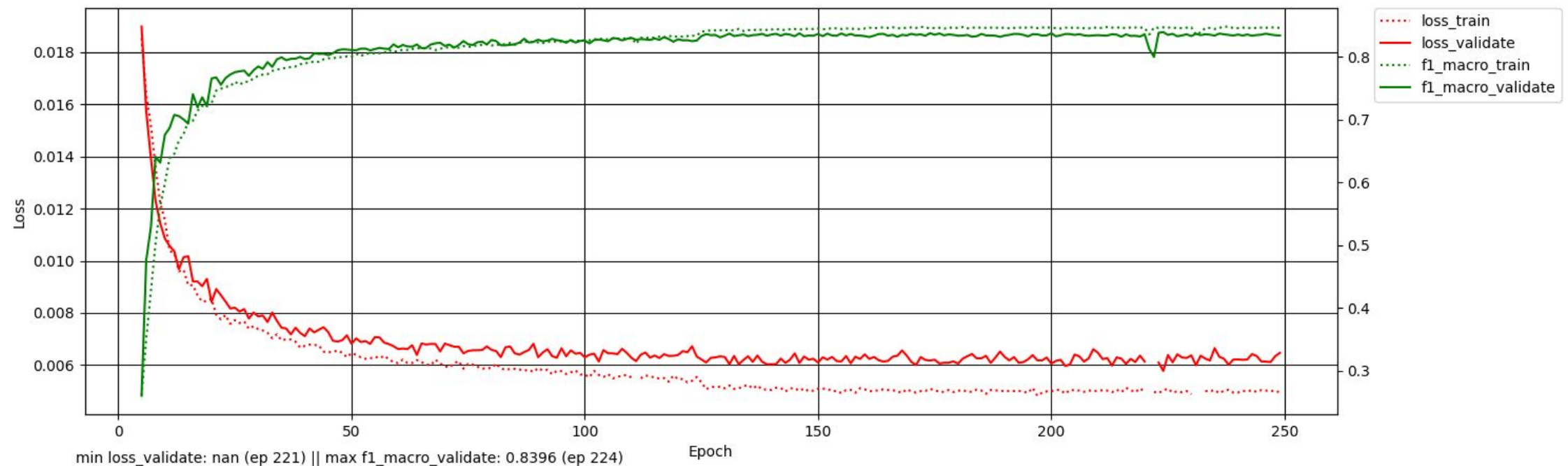
*"This is only training the first FCNN. Also the TractSeg version you can download via pip is also only using the first FCNN. The second one gives only very minor improvements but increases runtime a lot. Therefore, I actually never use it."*

# Loss - peaks

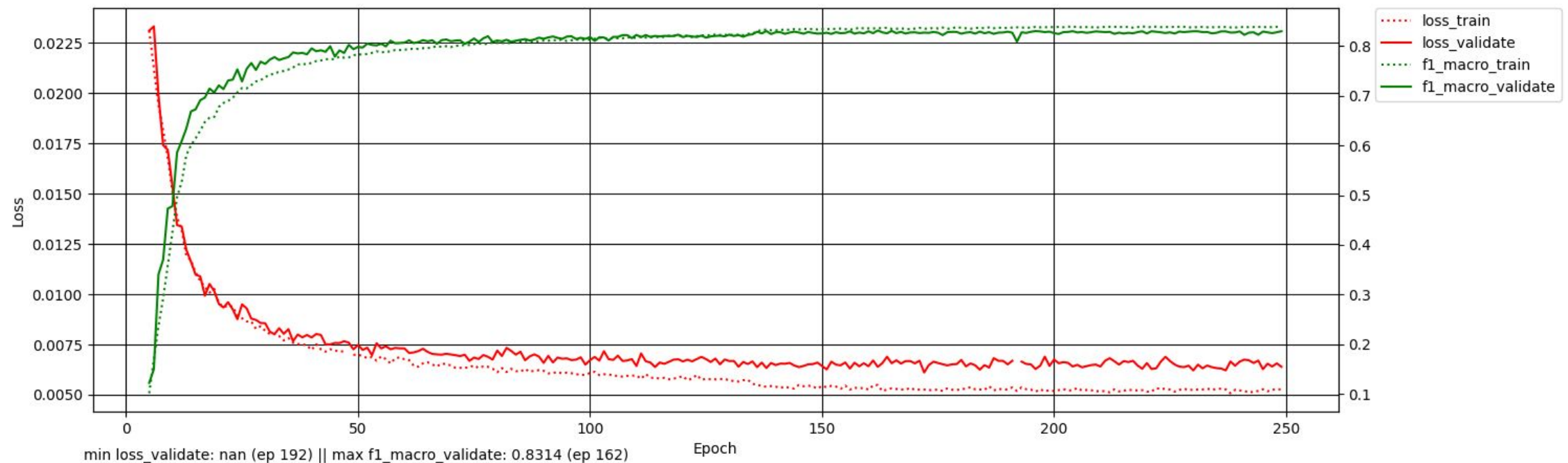
---



# Loss - fODF tensors



# Loss - rank-3 approximation



# Overfitting with fODFs

- Experiment without data augmentation
- Overfitting effect mitigated by learning rate scheduler

